

644

645 **Supplemental figure legends**

646 **Supplemental Figure 1.** Phylogeny of Patients 1-4 with PAO1 and PA14. Patients 1, 2, and 4

647 cluster with PAO1, while Patient 3 clusters with PA14.

648  
649 **Supplemental Figure 2.** Linear regression analysis demonstrates that total SNP count in a  
650 population was a strong indicator of AMR diversity for amikacin ( $R^2 = .90$ ,  $F(1, 2) = 18.94$ ,  $p =$   
651  $.049$ ), meropenem ( $R^2 = .93$ ,  $F(1, 2) = 25.3$ ,  $p = .037$ ), and piperacilin-tazobactam ( $R^2 = .95$ ,  $F(1,$   
652  $2) = 39.86$ ,  $p = .024$ ), but a poor indicator of AMR diversity for ciprofloxacin ( $R^2 = .12$ ,  $F(1,2) =$   
653  $.27$ ,  $p = .65$ ) and ceftazidime ( $R^2 = .71$ ,  $F(1,2) = 4.78$ ,  $p = .16$ ), and was inversely related to AMR  
654 diversity for tobramycin ( $R^2 = .97$ ,  $F(1,2) = 66.61$ ,  $p = .015$ )

655  
656 **Supplemental Figure 3.** Linear regression analysis shows that the number of distinct CARD  
657 profiles within a population is an improved predictor of population standard deviation for  
658 ciprofloxacin ( $R^2 = .79$ ,  $F(1,2) = 7.35$ ,  $p = .11$ ), tobramycin ( $R^2 = .77$ ,  $F(1,2) = 6.73$ ,  $p = .12$ ), and  
659 ceftazidime ( $R^2 = .81$ ,  $F(1,2) = 8.44$ ,  $p = .10$ ) over total population SNP count.

660  
661 **Supplemental Figure 4.** Enrichment analysis of the frequency of functional categories in which  
662 non-synonymous SNPs and microindels are found in each of the four populations relative to the  
663 proportions of these functional categories in the PAO1 genome shows that protein secretion/  
664 export apparatuses and transcriptional regulators are enriched for such variants, while phage/  
665 transposon/ plasmid and non-coding RNA are less likely to be impacted by such variants. Donut  
666 plot of the relative frequencies of genes categorized within each of the 27 different PseudoCAP  
667 functional categories in the PAO1 genome (A). Donut plots of the relative frequencies of non-  
668 synonymous SNPs and indels located in each of the 27 different PseudoCAP functional  
669 categories in Patient 1 (B), 2 (C), 3 (D), and 4 (E). Protein secretion/ export apparatuses and  
670 transcriptional regulators are denoted with green asterisks on donut plots where applicable, while  
671 phage/ transposon/ plasmid and non-coding RNA are denoted with red asterisks.

672  
673 **Supplemental Figure 5.** Principal components analysis vectors display no evidence of collateral  
674 sensitivity across any of the six antimicrobials tested for any patient, and further demonstrate that  
675 cross-resistance and cross-sensitivity patterns differ across patients.

676  
677 **Supplemental Figure 6.** Scatterplots of zone of inhibition (ZOI) versus growth rate ( $r$ ) in SCFM  
678 for all six tested antibiotics: amikacin (AK), meropenem (MEM), piperacillin-tazobactam (TZP),  
679 ciprofloxacin (CIP), tobramycin (TOB), and ceftazidime (CAZ). Results of linear mixed model  
680 (Table S18), with growth rate in SCFM as a fixed effect and patient as a random effect,

681 demonstrate that there is no significant effect of growth rate on resistance, and therefore, no  
682 evidence for trade-offs between growth rate and resistance in these four populations.

683

684 **Supplemental Table 1.** Antimicrobial susceptibility testing measurements for Patient 1 as  
685 measured by zone of inhibition (ZOI) in a standard disc diffusion assay for amikacin (AK),  
686 meropenem (MEM), piperacilin-tazobactam (TZP), ciprofloxacin (CIP), tobramycin (TOB), and  
687 ceftazidime (CAZ). Data in the left columns represent raw measurements of zone of inhibition  
688 radii (mm units). Data in the right columns represent calculated zone of inhibition values as  
689 diameters (mm units).

690

691 **Supplemental Table 2.** Antimicrobial susceptibility testing measurements for Patient 2 as  
692 measured by zone of inhibition (ZOI) in a standard disc diffusion assay for amikacin (AK),  
693 meropenem (MEM), piperacilin-tazobactam (TZP), ciprofloxacin (CIP), tobramycin (TOB), and  
694 ceftazidime (CAZ). Data in the left columns represent raw measurements of zone of inhibition  
695 radii (mm units). Data in the right columns represent calculated zone of inhibition values as  
696 diameters (mm units).

697

698 **Supplemental Table 3.** Antimicrobial susceptibility testing measurements for Patient 3 as  
699 measured by zone of inhibition (ZOI) in a standard disc diffusion assay for amikacin (AK),  
700 meropenem (MEM), piperacilin-tazobactam (TZP), ciprofloxacin (CIP), tobramycin (TOB), and  
701 ceftazidime (CAZ). Data in the left columns represent raw measurements of zone of inhibition  
702 radii (mm units). Data in the right columns represent calculated zone of inhibition values as  
703 diameters (mm units).

704

705 **Supplemental Table 4.** Antimicrobial susceptibility testing measurements for Patient 4 as  
706 measured by zone of inhibition (ZOI) in a standard disc diffusion assay for amikacin (AK),  
707 meropenem (MEM), piperacilin-tazobactam (TZP), ciprofloxacin (CIP), tobramycin (TOB), and  
708 ceftazidime (CAZ). Data in the left columns represent raw measurements of zone of inhibition  
709 radii (mm units). Data in the right columns represent calculated zone of inhibition values as  
710 diameters (mm units).

711

712 **Supplemental Table 5.** Genome size, average sequencing coverage, and number of contigs of  
713 each assembly.

714

715 **Supplemental Table 6.** Supporting statistical values of the linear regression analysis of distinct  
716 CARD resistance genotype profiles within a population as a proxy for genomic diversity as  
717 measured by total SNPs in each population.

718

719 **Supplemental Table 7.** Genes that were impacted by non-synonymous mutations in at least one  
720 isolate in all four populations.

721

722 **Supplemental Table 8.** Full details of the chi-squared goodness of fit and Monte Carlo simulation  
723 exact multinomial tests, with all associated chi-squared and p-values.

724

725 **Supplemental Table 9.** Genes that were impacted by non-synonymous mutations in at least one  
726 isolate in three out of four populations.

727

728 **Supplemental Table 10.** All annotated genetic variants discovered in Patient 1.

729

730 **Supplemental Table 11.** All annotated genetic variants discovered in Patient 2.

731

732 **Supplemental Table 12.** All annotated genetic variants discovered in Patient 3.

733

734 **Supplemental Table 13.** All annotated genetic variants discovered in Patient 4.

735

736 **Supplemental Table 14.** Raw OD<sub>600</sub> reads for growth in SCFM used to create growth curves and  
737 analyze growth rate (r) for Patient 1. Time is given in hours, and all isolates were tested in  
738 biological triplicates.

739

740 **Supplemental Table 15.** Raw OD<sub>600</sub> reads for growth in SCFM used to create growth curves and  
741 analyze growth rate (r) for Patient 2. Time is given in hours, and all isolates were tested in  
742 biological triplicates.

743

744 **Supplemental Table 16.** Raw OD<sub>600</sub> reads for growth in SCFM used to create growth curves and  
745 analyze growth rate (r) for Patient 3. Time is given in hours, and all isolates were tested in  
746 biological triplicates.

747

748 **Supplemental Table 17.** Raw OD<sub>600</sub> reads for growth in SCFM used to create growth curves and  
749 analyze growth rate (r) for Patient 4. Time is given in hours, and all isolates were tested in  
750 biological triplicates.

751

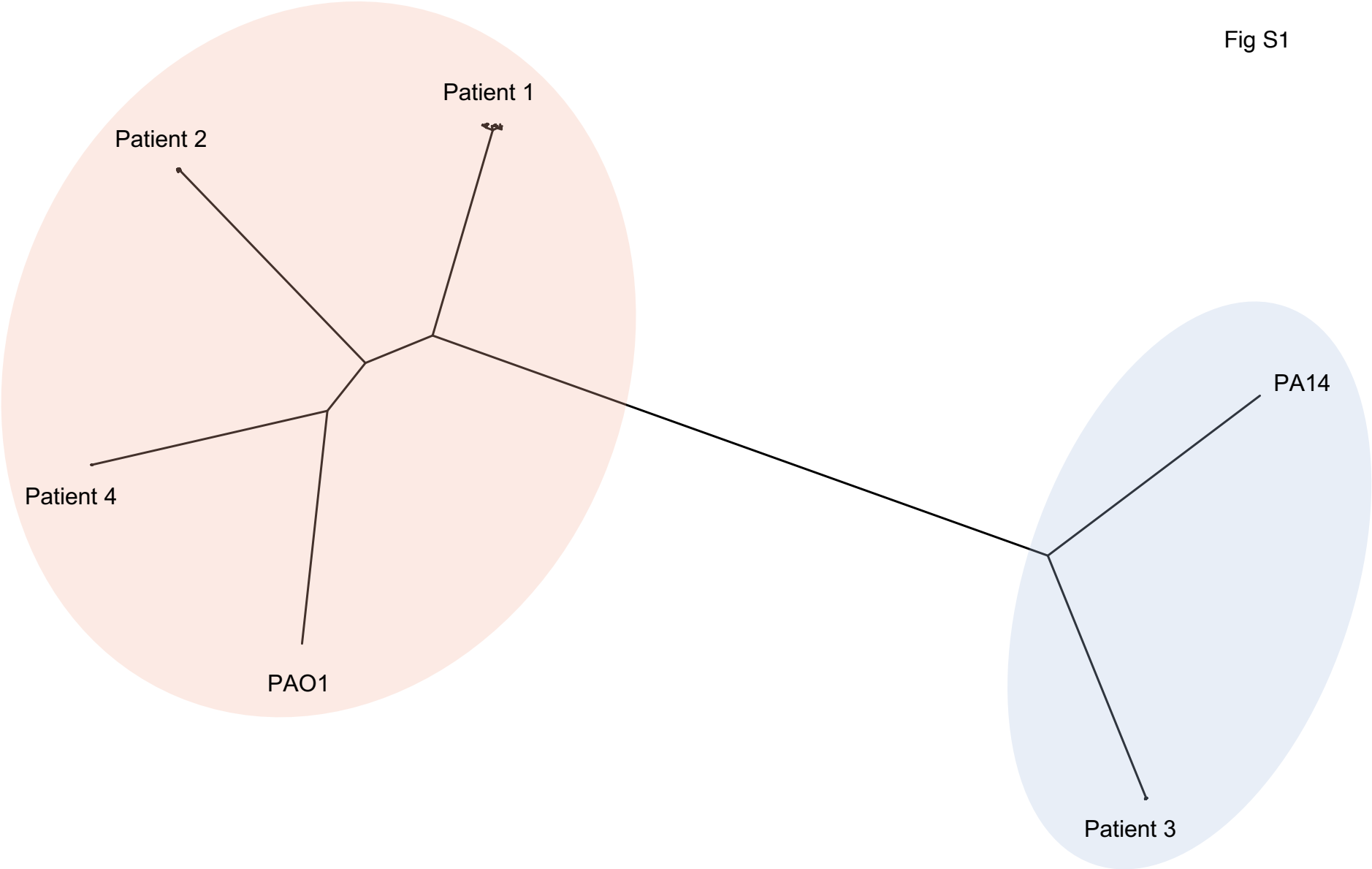
752 **Supplemental Table 18.** Supporting brms R code and statistical values for the linear mixed model  
753 run to assess the relationship between growth rate (r) and antimicrobial resistance. Results of the  
754 model, with growth rate in SCFM as a fixed effect and patient as a random effect, show that the  
755 95% confidence interval of the fixed effect of growth rate spans 0 for all six antimicrobials.  
756 Therefore, the null hypothesis that the fixed effect of growth on antimicrobial susceptibility is 0  
757 cannot be rejected, providing no evidence for trade-offs or any significant relationship between  
758 resistance and growth rate across all four populations.

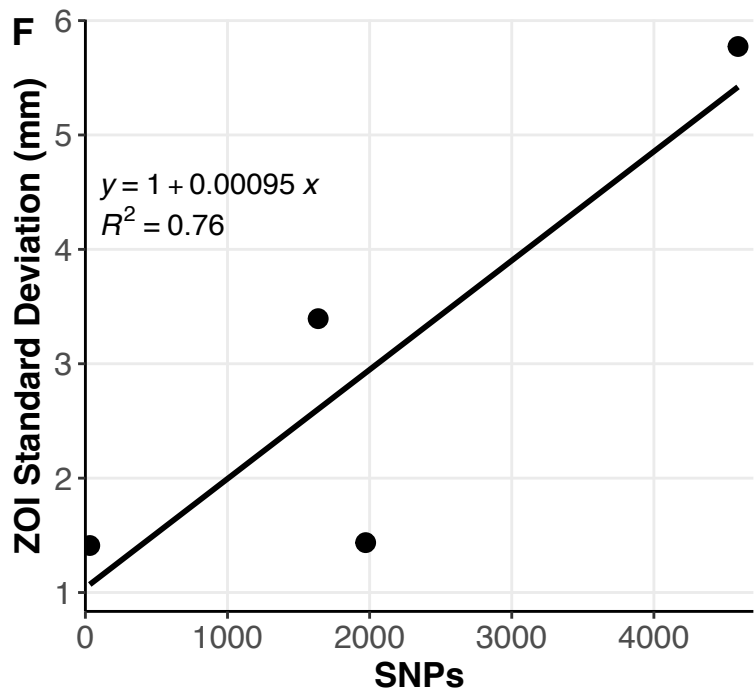
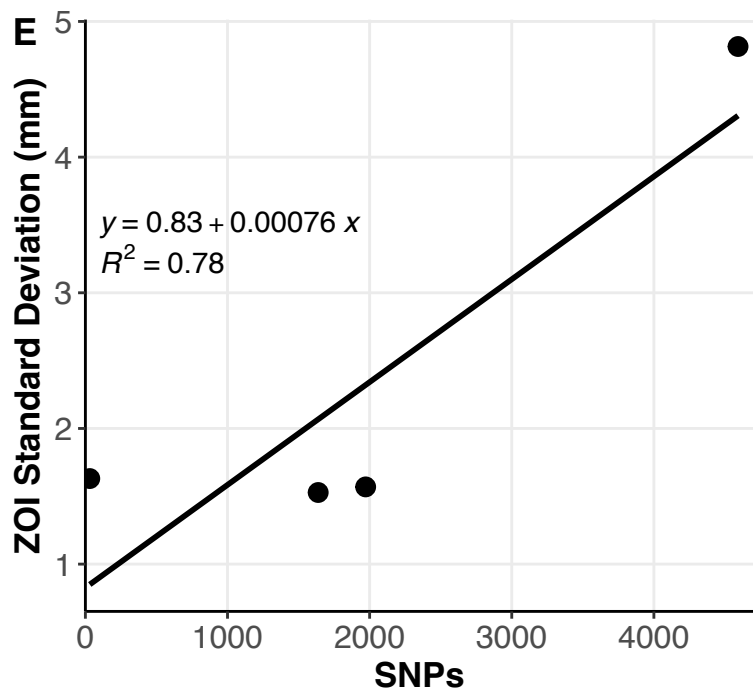
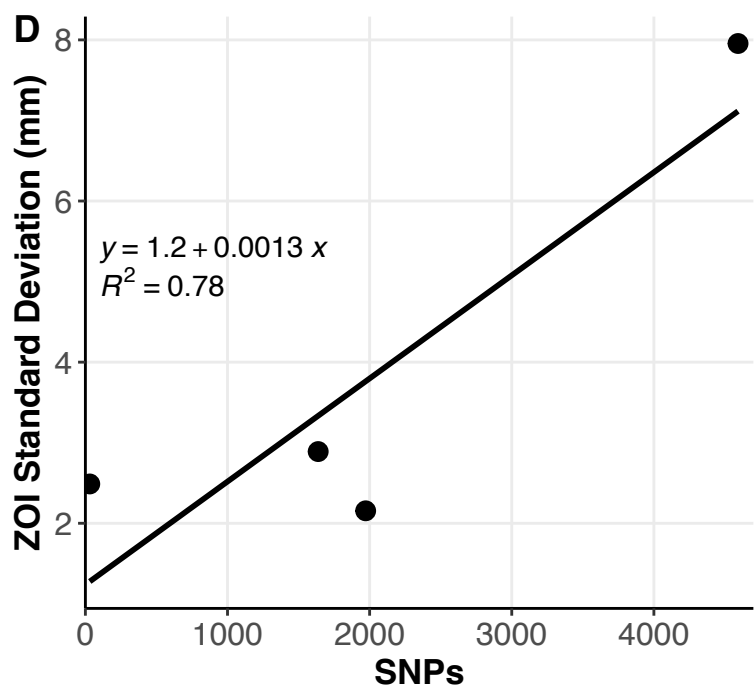
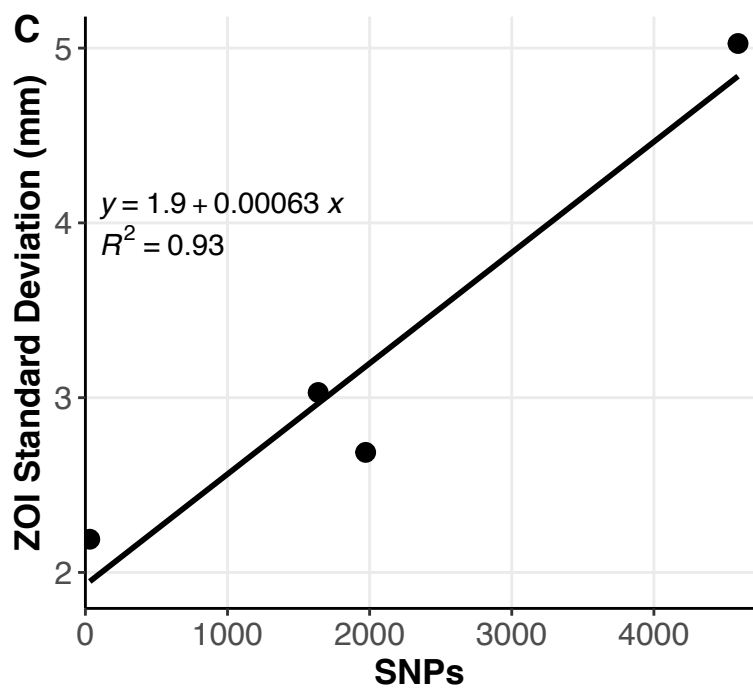
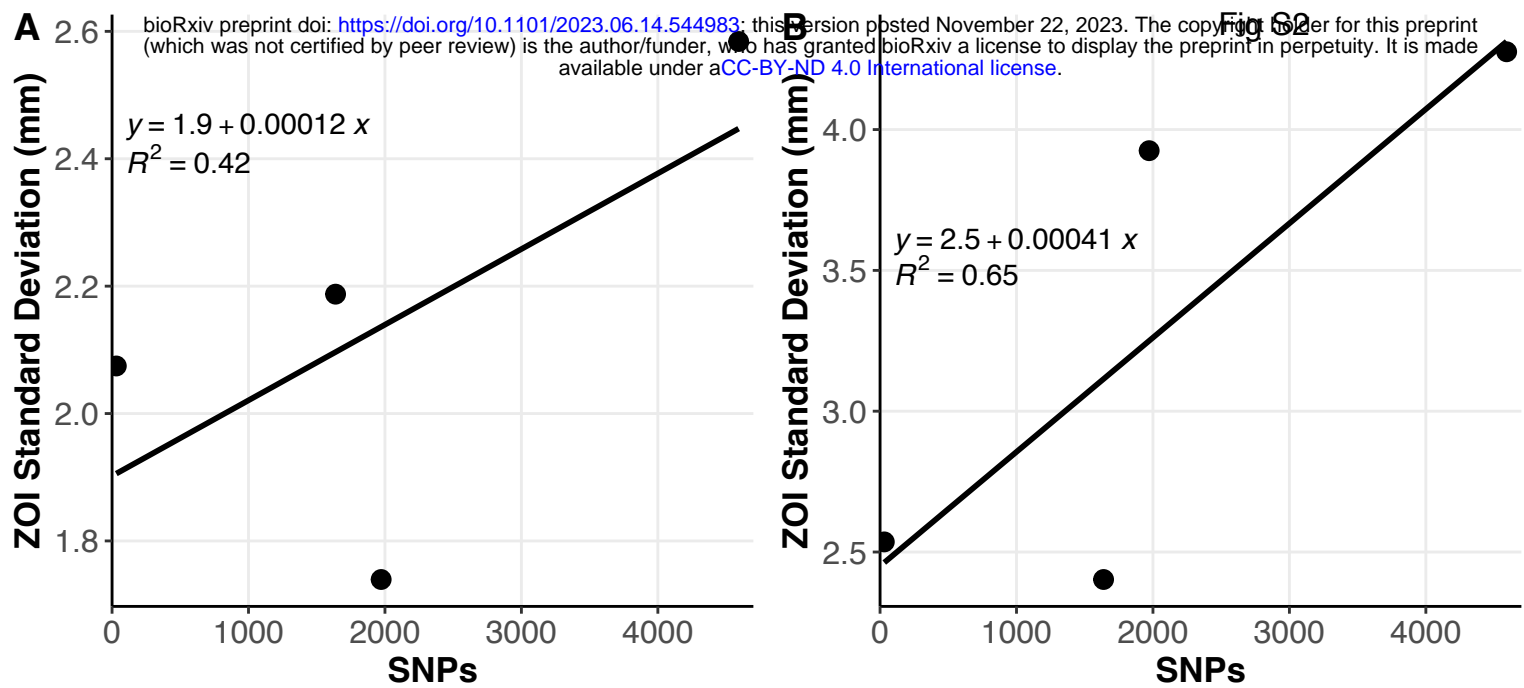
759

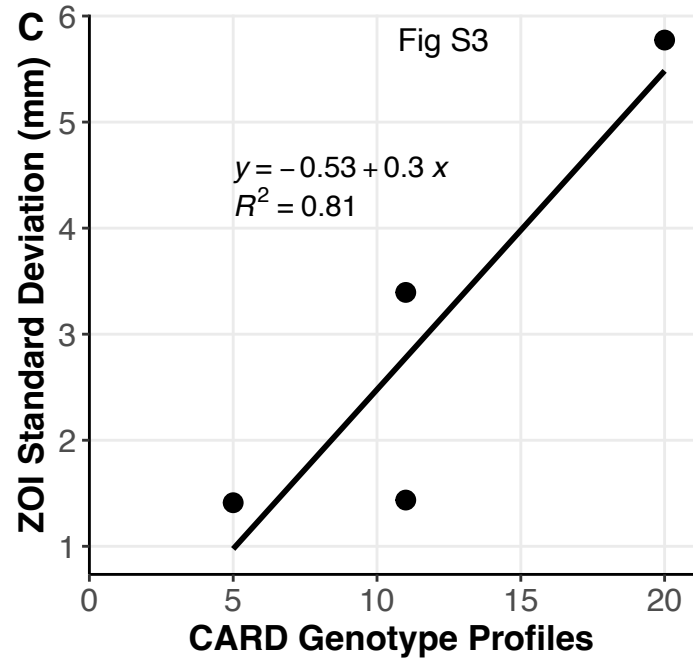
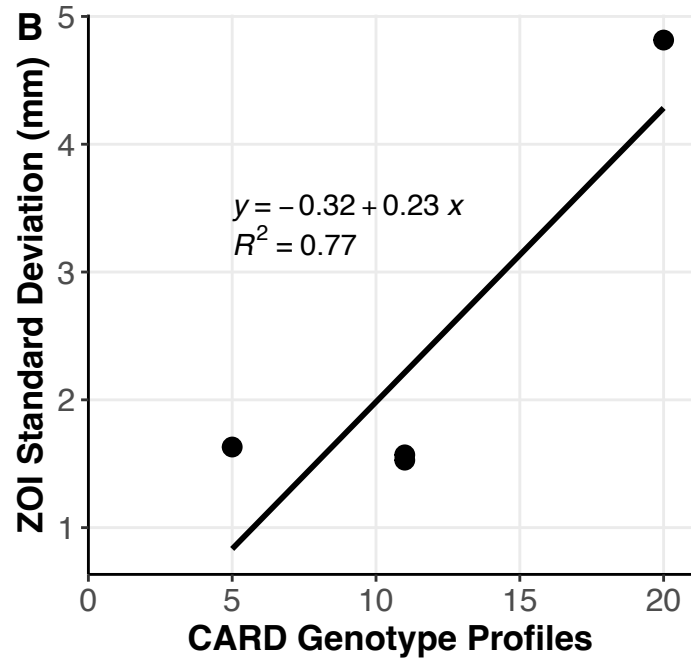
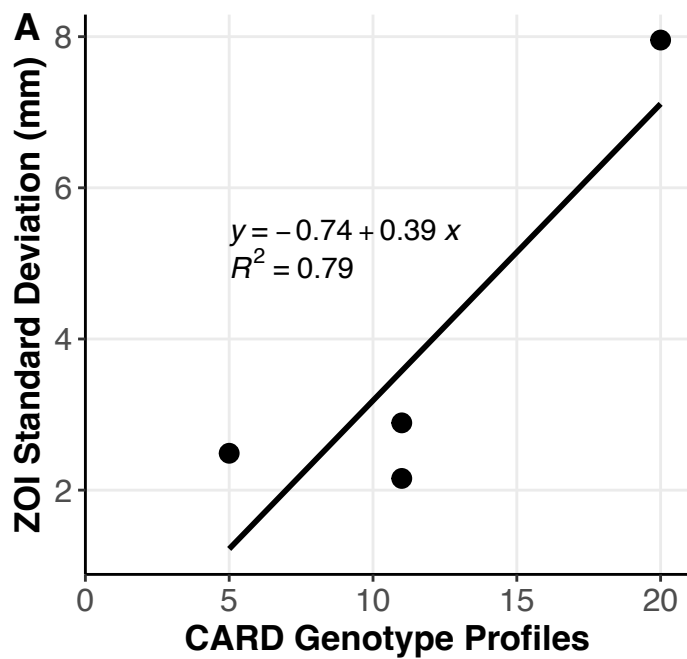
760

761

Fig S1









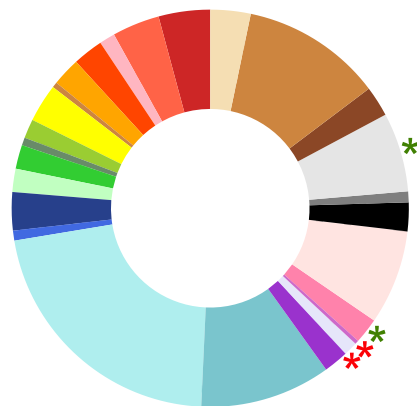
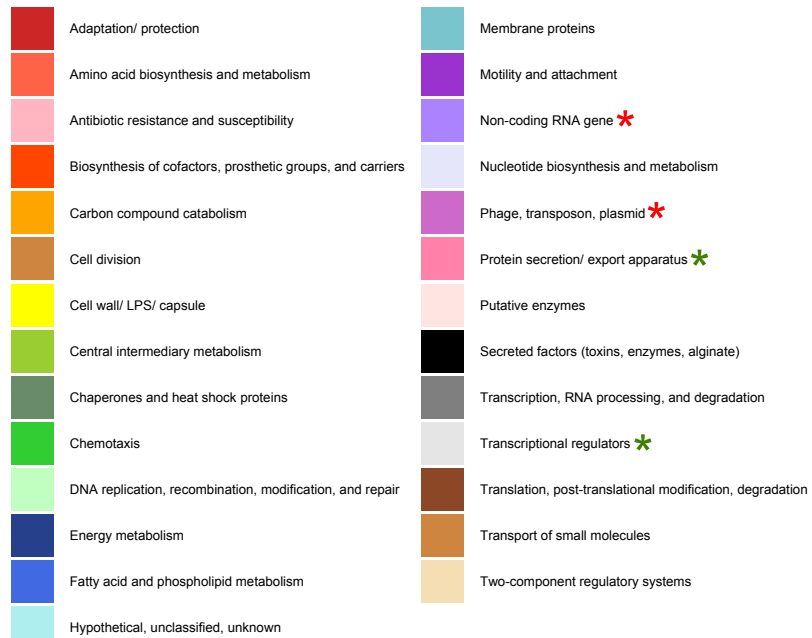
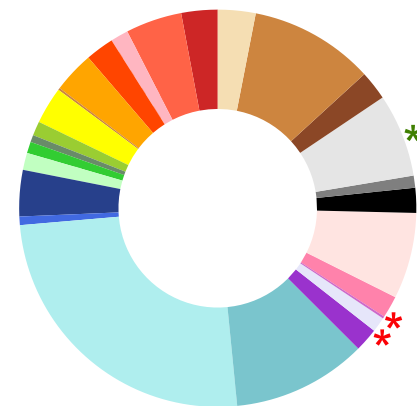
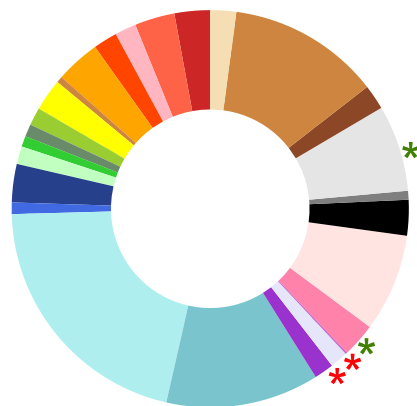
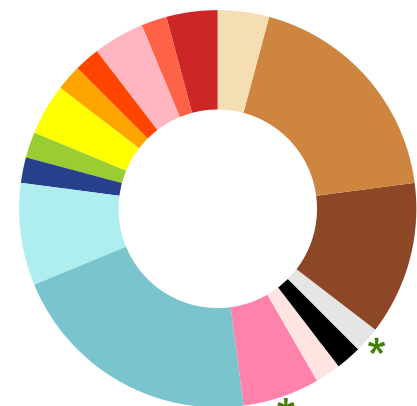
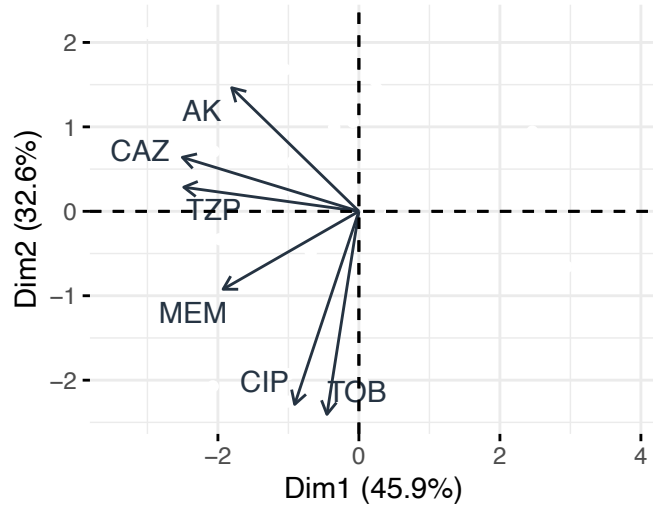
**A****B****C**

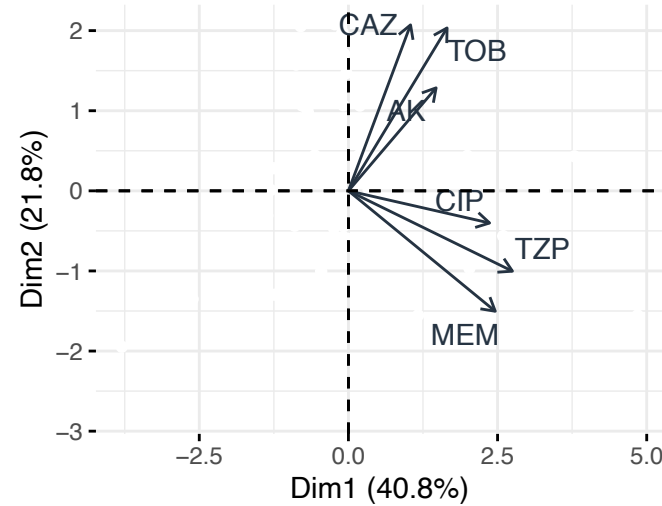
Fig S4

**D****E**

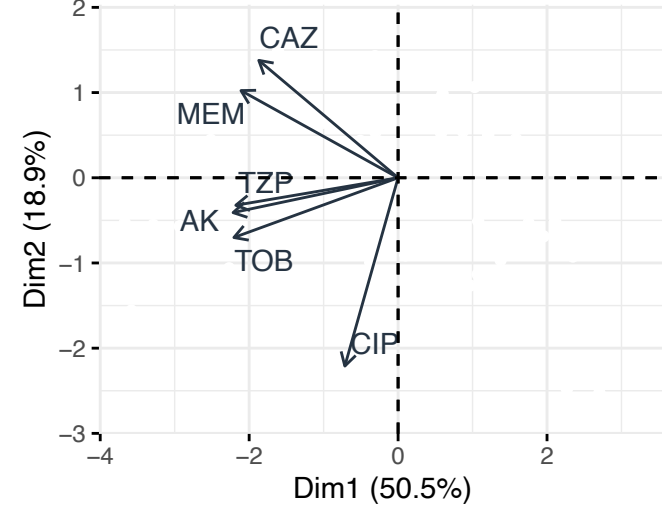
**Patient 1** Fig S5



**Patient 2**



**Patient 3**



**Patient 4**

